Protist, Vol. 165, 343–363, May 2014
http://www.elsevier.de/protis
Published online date 18 April 2014

Protist

ORIGINAL PAPER

Ribosomal DNA Organization Patterns within the Dinoflagellate Genus *Alexandrium* as Revealed by FISH: Life Cycle and Evolutionary Implications

Rosa Isabel Figueroa[a,b,1], Angeles Cuadrado[c], Anke Stüken[d], Francisco Rodríguez[b], and Santiago Fraga[b]

[a]Aquatic Ecology, Biology Building, Lund University, 22362 Lund, Sweden
[b]Instituto Español de Oceanografía (IEO), Subida a Radio Faro 50, 36390 Vigo (Spain)
[c]Universidad de Alcalá (UAH), Dpto de Biomedicina y Biotecnología, 28801 Alcalá de Henares (Spain)
[d]Microbial Evolution Research Group, Department of Biosciences, University of Oslo, P.O. Box 1066, Blindern, 0316 Oslo (Norway)

Submitted September 10, 2013; Accepted April 8, 2014
Monitoring Editor: Marina Montresor

Dinoflagellates are a group of protists whose genome differs from that of other eukaryotes in terms of size (contains up to 250pg per haploid cell), base composition, chromosomal organization, and gene expression. But rDNA gene mapping of the active nucleolus in this unusual eukaryotic genome has not been carried out thus far. Here we used FISH in dinoflagellate species belonging to the genus *Alexandrium* (genome sizes ranging from 21 to 170 pg of DNA per haploid genome) to localize the sequences encoding the 18S, 5.8S, and 28S rRNA genes. The results can be summarized as follows: 1) Each dinoflagellate cell contains only one active nucleolus, with no hybridization signals outside it. However, the rDNA organization varies among species, from repetitive clusters forming discrete nuclear organizer regions (NORs) in some to specialized "ribosomal chromosomes" in other species. The latter chromosomes, never reported before in other eukaryotes, are mainly formed by rDNA genes and appeared in the species with the highest DNA content. 2) Dinoflagellate chromosomes are first characterized by several eukaryotic features, such as structural differentiation (centromere-like constrictions), size differences (dot chromosomes), and SAT (satellite) chromosomes. 3) NOR patterns prove to be useful in discriminating between cryptic species and life cycle stages in protists.

Key words: Chromosomes; genome size; Nuclear Organizer Regions (NORs); protists; ribosomal genes; life cycle.

Introduction

Dinoflagellates comprise a large group of flagellate protists well known for causing harmful algal blooms in coastal waters worldwide (Anderson et al. 1998). Member species differ greatly in their

[1]Corresponding author;
e-mail rosa.figueroa@biol.lu.se, Rosa.Figueroa@vi.ieo.es (R.I. Figueroa).

http://dx.doi.org/10.1016/j.protis.2014.04.001

morphology, nutritional habits, and habitats and may be planktonic, benthic, heterotrophic, autotrophic, or parasitic. The high abundance of photosynthetic dinoflagellates make this group of phytoplankton first, important primary producers, and second, an important component of the microbial loop and of coral symbionts (Hackett et al. 2004). Their complex life cycle, which includes ploidy and planktonic-benthic shifts, is in part responsible for their ecological success. Vegetative stages (planktonic) divide asexually by mitosis. But under certain conditions they enter the sexual cycle through gamete fusion, giving rise to zygotes that either divide and remain planktonic or become benthic, dormant cysts (Pfiester and Anderson 1987).

The specialized nucleus of dinoflagellates is referred to as the dinokaryon (Rizzo 1991). Chromatin in the dinokaryon is permanently organized as a cholesteric liquid crystal structure (Chow et al. 2010; Rill et al. 1989), so that, under the light microscope, chromosomes appear condensed throughout the cell cycle. Chromosomal replication and division proceeds via closed mitosis, as the nuclear envelope does not break down and the mitotic spindle is extranuclear (Soyer-Gobillard et al. 1999). Consistent with the huge size of their genome (up to 250pg), dinoflagellates have one of the highest number of chromosomes among eukaryotes, with some species containing up to 143 chromosomes in the haploid state (see Hackett et al. 2004 and references therein). As in other eukaryotes, dinoflagellate chromosomes are linear (Alverca et al. 2007) and with telomeres which form the longest tandem array thus far observed in unicellular organisms (Fojtová et al. 2010). Histones were long considered to be absent, but despite the very low protein/DNA ratio (1:10) (Kellenberger 1988), all core histone transcripts were identified (Lin et al. 2010; Roy and Morse 2012). Whereas chromosomal decondensation does not occur in dinoflagellates, large variations in the birefringence and optical properties of their chromosomes have been reported among different species and between individual karyotypes (Chow et al. 2010). However, chromosome size, morphology (e.g. presence of primary or secondary constrictions), and the presence of eu-/heterochromatin regions have yet to be adequately described. Based on the absence of a dinokaryon in Perkinsozoa as well as in Oxyrrhinaceae and Syndiniales, the dinokaryon appears to be a derived rather than an ancestral nuclear configuration (Okamoto et al. 2012; Taylor et al. 2008). Nonetheless, the acquisition of this huge size together with the lack of nucleosomes and virtually no histone expression makes the dinokaryon a highly interesting model to study the processes determining genome size and stability in eukaryotes.

There appears to be a high degree of DNA redundancy in the dinoflagellate genome. Noncoding repetitive sequences comprise up to 60% of dinoflagellate genomes, have a distribution linked to the specific and atypical organization of the chromatin (Moreau et al. 1998) and are thought to be important to genome stability by contributing to the overall compactness of chromosomes (Jaeckisch et al. 2011). Regarding coding sequences, most of the dinoflagellate genes studied so far are organized in tandem repeats, a fact not common in other eukaryotes (e.g Hou and Lin, 2009; Lin 2011).

Ribosomal DNA (rDNA) is one of the most well-characterized coding arrays in eukaryotes (Hillis and Dixon 1991). rRNA genes are the most abundant and critical housekeeping genes in the eukaryotic genome (Chakraborty and Kenmochi 2012), which are those transcribed into the components of the ribosome. In plants and higher eukaryotes, rDNA regions containing the genes for the 18S, 5.8S, and 28S rRNAs (transcribed as the 45S ribosomal precursor), form the nucleolar organizer regions (NORs), whereas genes that make up the 5S rRNA are transcribed outside the NOR. Each nucleolar organizing region contains a cluster of tandemly repeated rRNA genes that are separated from each other by non-transcribed spacer DNA. The evolutionary variation in the nuclear genome among species can be tracked by following NOR clusters, which behave as neutral genetic markers because their number and position are often species-specific (Britton-Davidian et al. 2012). Accordingly, NORs have been widely used in systematics and in phylogenetic reconstructions (see for e. g. in plants Carvalho et al. (2011); in fishes Frolov and Frolova (2004); and in amphibians Reinaldo Cruz Campos et al. (2009)). Studies on NOR variation in numerous plant, insect, and vertebrate groups have invariably described changes in the number and chromosomal location of the NORs even in closely related species, suggesting that rDNA clusters are highly mobile genomic components (Britton-Davidian et al. 2012 and references therein).

In the present work, we used fluorescence in situ hybridization (FISH) to investigate the organization of the NOR and its possible relation to genome size in species of the dinoflagellate genus *Alexandrium*. These species occur in marine waters worldwide

and include those able to cause the neurotoxic syndrome PSP (Paralytic Shellfish Poisoning) (e.g. Anderson et al. 2012). *Alexandrium* genome sizes range from 21.8 pg per haploid cell in *A. andersonii* to more than 100 pg in strains of the *Alexandrium tamarense/catenella/fundyense* species complex (LaJeunesse et al. 2005); however, essentially nothing is known about species-specific differences in the organization of these large genomes. We therefore studied chromosomal rDNA localization in 16 strains belonging to the species *A. affine*, *A. margalefii*, *A. andersonii*, *A. minutum* and the A. *tamarense/catenella/fundyense* species complex, which includes cryptic species (John et al. 2003; Lilly et al. 2007; Scholin et al. 1994; Wang et al. 2014). The chosen species differ greatly in the sizes of their genomes and in their phylogenetic positions, based on ribosomal ITS sequences. While in mammals, birds, and plants, mitochondrial genes are used in DNA barcoding, for protists, ribosomal genes have been shown to be more appropriate (Pawlowski et al. 2012).

Phylogenetic studies of *Alexandrium* have contradicted several morphological classifications of the species within this genus. Several clades (ribotypes) that could not be assigned to the species *A. tamarense*, *A. catenella*, and *A. fundyense* were identified, resulting in a designation of the "*A. tamarense/catenella/fundyense* species complex"(John et al. 2003; Scholin et al. 1994), later proposed to be named as Groups I to V by Lilly et al. (2007), or Groups I to IId (Miranda et al. 2012; Wang et al. 2014). Both classifications are equivalent and their differences lie in the designation of the groups. *A. affine*, a well characterized species, is a close relative both morphologically and phylogenetically to the groups I-V of the species complex (Lilly et al. 2007; Scholin et al. 1994).

Our results show clear differences in the NOR organizational patterns of the *Alexandrium* species studied. Furthermore, we found that in some

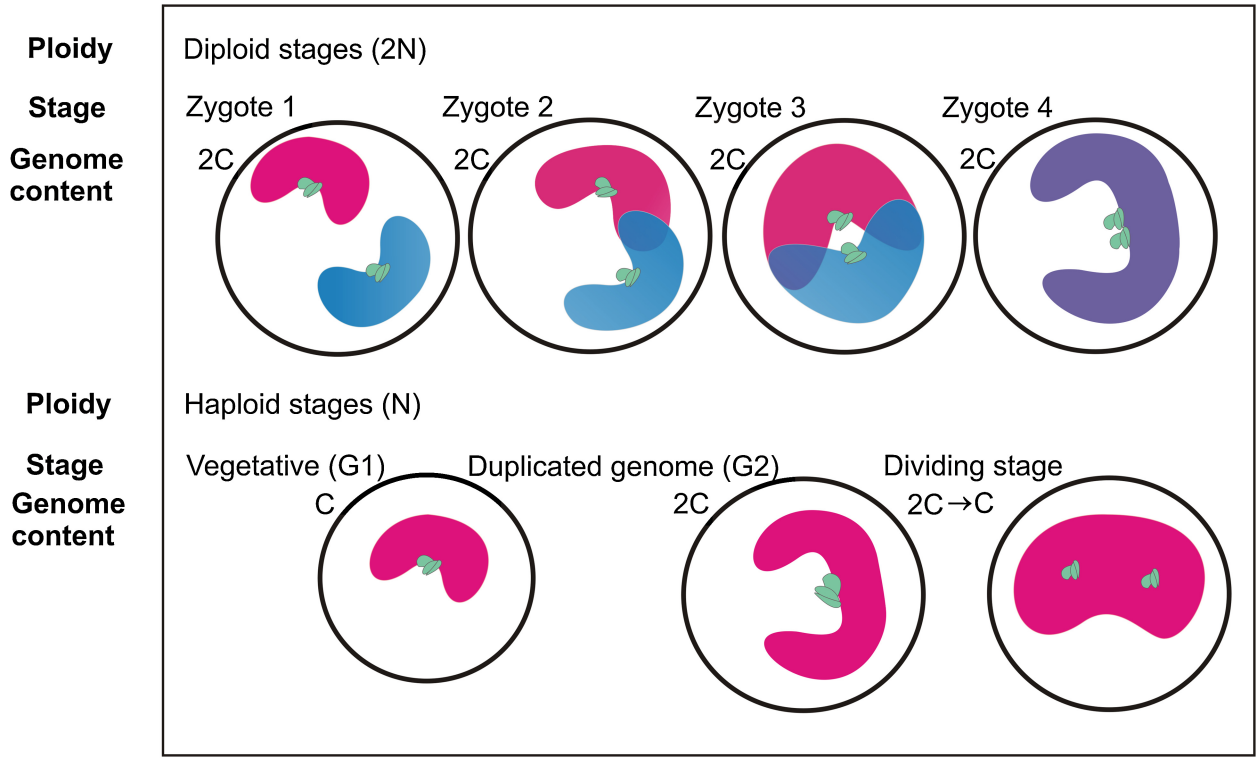

Figure 1. Nuclear shapes, cell cycle stages and ploidity during the sexual and asexual cycle of *A. minutum* (sexual fusion according to Figueroa et al. (2006)). The ribosomal genes (shown in green) are located central to the nuclei. In "zygote 1" the U-shaped nuclei have not yet fused. In "zygote 2" and "zygote 3" fusion starts at one of the nuclear arms and, a few hours later, continues in the other. The fused nuclei typically acquire a "doughnut" shape. "Zygote 4" is a fully formed zygote, with a noticeably larger nucleus and a double set of ribosomal genes. Asexual stages are shown below: Two vegetative stages (G1 and G2) and a mitotic stage (dividing cell). Stages with duplicated genome (2C genome content) as G2 stages and mature zygotes (2N, diploid) are not possible to differentiate unambiguously.

Alexandrium minutum

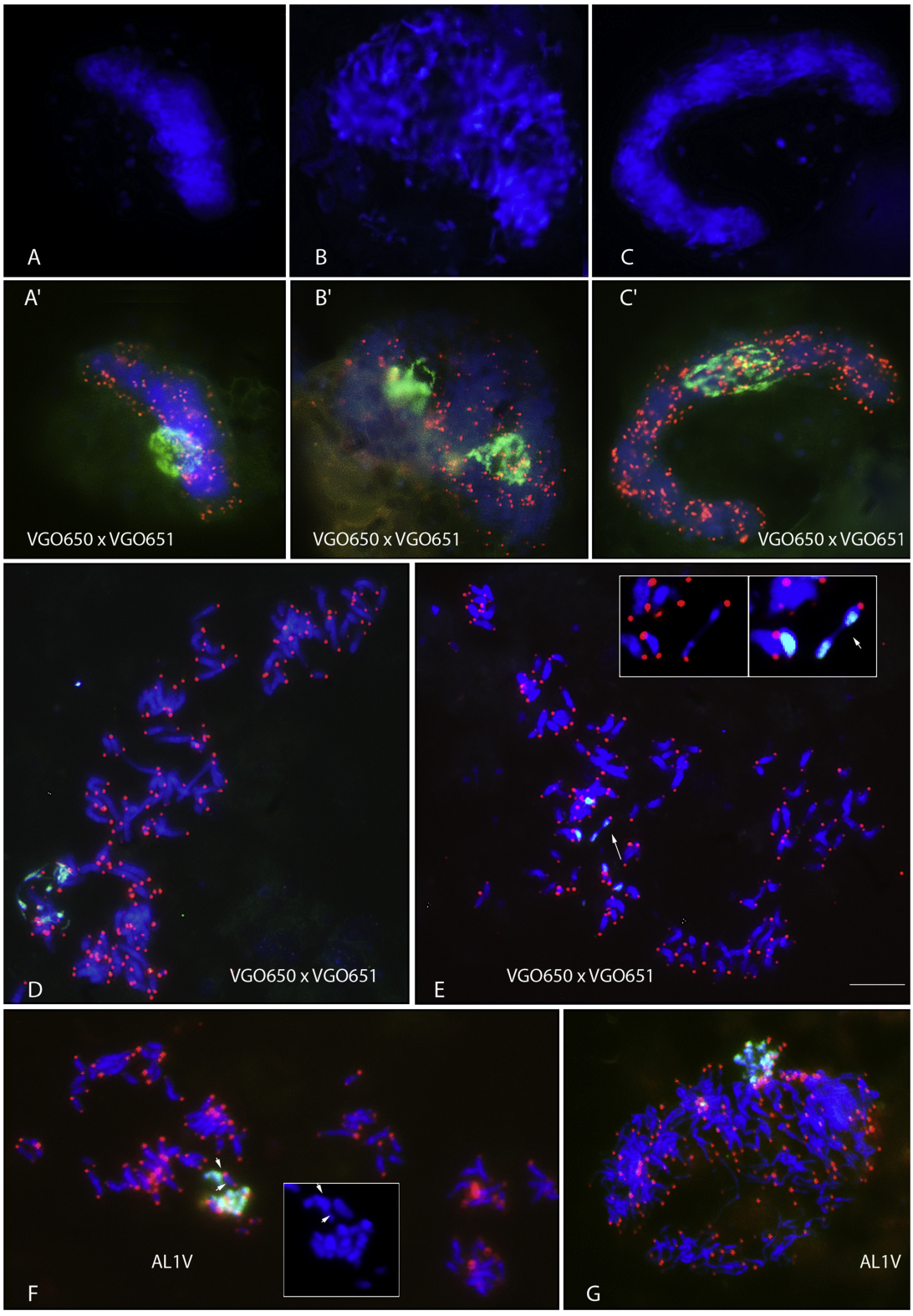

species rRNA genes are organized within what could be considered in a broad sense as "ribosomal chromosomes", because ribosomal genes compose most of their content. To our knowledge, these specialized chromosomes have never been reported in other eukaryotes. Their presence is not related to the phylogenetic position of the species nor unequivocally to genome size. However, they were detected in all species with the highest DNA content. The function of this atypical dinoflagellate chromosome structure is discussed herein, as is the utility of using NOR patterns to reveal cryptic species and for life-cycle stage discrimination.

Results

Genome Size Content

The species included in the study showed a broad range of genome sizes, from the 21–26 pg of DNA per vegetative nucleus of *A. andersonii* (22.0±0.6) and *A. minutum* (25.3±3.2) to the 98.2±4.1 and 169.0±3.21 pg of DNA per vegetative cell of *A. affine* and *A. margalefii* respectively. The broadest variability occurred in the *Alexandrium tamarense/catenella/fundyense* species complex (64.7±7.7 pg), as evidenced by the highest standard deviation.

Diversity in Genome Size and NOR Patterns within the Genus *Alexandrium*

Independent of the NOR organization, all *Alexandrium* species studied contained a single large nucleolus. In the following, we describe the results for each species, from the smallest to the largest with respect to genomic content.

Alexandrium minutum

To identify and classify the possible sources of intraspecies variability in NOR patterns, we studied both asexual and sexual cultures of *Alexandrium minutum*. In this species, the chosen strains do not produce sexual stages during clonal growth but can be induced to do so under certain nutrient conditions (Figueroa et al. 2007, 2011). Since the other species included in this work are able to self-fertilize (homothallism) to produce both asexual and sexual stages during clonal growth (Anderson et al. 2012), but not the studied *A. minutum* strains (Figueroa et al. 2007), we chose *A. minutum* to look for possible sexually related NOR patterns. Figure 1 shows the sequence of nuclear transformations during zygote formation in the U-shaped nuclei of *Alexandrium* (Figueroa et al. 2006), including the behavior of the ribosomal genes. Fusing gametes and mobile zygotes (planozygotes) show the presence of two nuclei (zygote 1), later a nucleus that is doubled in size and with a double set of ribosomal genes (zygote 2 and zygote 4), going through an intermediate nuclear stage with a typical doughnut shape in phase 3. On the contrary, vegetative cells (G1) have one U-shaped nucleus. During the mitotic cycle, cells that have duplicated their genome and are arrested in G2 are larger in size and with larger nuclei and nucleoli. Cells undergoing division change nuclear morphology, showing more roundish nuclei and two sets of ribosomal genes.

The most common nuclear morphology observed in a sexually induced *A. minutum* culture (Fig. 2A–E) was typically U-shaped, presumably corresponding to the nucleus of an interphasic vegetative cell (Fig. 2A). Cells with two nucleoli of the same size were also observed in low frequencies (Fig. 2B). Apparently, the nucleoli were similar in size to the nucleolus shown in Figure 2A but the chromosomes are more condensed which suggests that these cells are undergoing division. A recent gamete fusion could not be totally ruled out. Figure 2C depicts a stage 4 planozygote (Fig. 1), judged by the single nucleolus that is significantly larger than the one in the haploid stage (Fig. 2A) and the extended nuclear morphology consistent with that of a planozygote (Figueroa et al. 2007). However, a cell in the G2 stage of the cell cycle could not be totally discarded. In clonal strain AL1 V (Fig. 2F–G), the presence of mitotic metaphases is coherent with the detection of this nuclear morphology both in sexual (Fig. 2D, E) and asexual (Fig. 2F, G) cultures. The images show highly individualized chromosomes, organized nucleolus, and the

Figure 2. DNA DAPI staining (blue) and in situ hybridization of the digoxigenin-labeled pTa71 probe for the detection of ribosomal genes (green) and of the Dy547-labeled oligonucleotide $(CCCTAAA)_3$ for telomere localization (red) in *Alexandrium minutum* cells. When not all probes are shown simultaneously, a single letter applies to photos in which only DAPI staining has been used and (') refers to the result with all probes. (**A**) Vegetative nuclei; (**B**) dividing stage, (**C**) putative zygote or cell in G2 stage; (**D–G**) metaphase (see text). The cultures used were a sexual cross between VGO650 and VGO651 (A–E) and a clonal culture of AL1 V (F, G). Scale bars: 10 μm.

associated NOR. It is remarkable that rDNA occupies most of the length in two of the chromosomes (Fig. 2E, insert). The telomere signals at both chromosome ends define the chromosomal length and morphology, ruling out misidentifications with satellite structures. Clearly, chromosomes of different sizes are present. The longest chromosome shows no rDNA hybridization and weaker DAPI staining (DAPI negative or DAPI-) in the middle, a feature suggestive of the constrictions associated with centromeres in higher eukaryotes. Secondary constrictions associated with the NOR are seen in the insert of Figure 2F (DAPI detail).

Alexandrium andersonii

In the *A. andersonii* (strain SZN-12) preparation, there is a noticeable aggregation of telomeric signals in connection with the nucleolus. Figure 3A shows a vegetative stage, in which the nuclear morphology is similar to that of *A. minutum* but the nucleolus is smaller. In Figure 3B, C, the nuclei are wider, the nucleoli are duplicated, and there is a larger number of telomeres than in the vegetative cell. However, there are important differences between the nucleus of the vegetative cell and these nuclei (Fig. 3C, E, F) with respect to DNA content, chromosomal condensation, and nucleolar organization state, all of which affect the NOR morphology. Specifically, the presence of a residual (Fig. 3E) or complete (Fig. 3F) nucleolar organization suggests that the morphology of chromosomes undergoing replication, transcription, or pairing differs from that generally observed in interphasic, vegetative cells. In addition, important size differences were observed between the chromosomes. The very small chromosomes (arrows) seen in the detailed view provided in Figure 3D are confirmed by the proximity of the telomeric signals. We refer to these chromosomes as “dot chromosomes,” following the *Drosophila* nomenclature. As in *A. minutum*, we verified that when chromosomal individualization was achieved (as shown in Fig. 3D), the telomeric signals are restricted to the chromosome ends, suggesting that there are no significant matches outside the telomeres. In the nucleolus, there was a surprisingly high density of telomeric sequences, as seen in Figure 3G.

Alexandrium tamarense/catenella/fundyense Species Complex

Group I strains used in this study were from different hemispheres. However, the patterns of their NOR distributions were similar (Fig. 4). The most prominent common characteristic of Group I strains was the distinct DAPI signature of chromosomes whose bodies are mainly comprised of ribosomal genes (e.g., Fig. 4C, insert). These chromosomes are strongly stained with DAPI and therefore are referred to as DAPI positive (DAPI+). A vegetative nucleus is depicted in Figure 4A. According to our model of zygote formation (Fig. 1), a zygote in the process of fusion might be shown in Figure 4B, whereas the larger number of telomeric signals and the nuclear size of the cell shown in Figure 4E suggest that it is a mature zygote or a cell in G2 stage. Figure 4D shows a cell possibly in zygote 2 stage (Fig. 1). Figure 4B, C, and E can distinguish individual chromosomes, identified as such on the basis of the telomeric sequences at both ends of the DAPI+ chromosomes. In these chromosomes, the main body is formed by rDNA, which is present in enormous copy numbers. In the insert of Figure 4C one of these chromosomes shows a centromere-like constriction.

Group II cultures (Fig. 5) showed the same peculiarities in the location of the ribosomal genes, i.e., in certain central chromosomes located in the concave region of the U-shaped nuclei and distinguished by their DAPI+ signature. Figure 5A shows a vegetative haploid nucleus with the NOR in a peripheral position. In the cell shown in Figure 5B, the nucleolus is fully developed, while Figure 5C, E highlights the co-localization of DAPI+ chromosomes and the ribosomal genes. The exception in this group was strain CNR-ATAA1 (Fig. 5D), which had comparatively fewer ribosomal gene copies and no DAPI+ chromosomes associated with the NOR. In Figure 5D the blurred green color all over the nucleus is due to the over-exposition needed to verify the lack of significant signals.

Strains from Groups III and IV (Fig. 6) similarly contained specific chromosomes for ribosomal genes, as described in Groups I and II. However, these chromosomes were not associated with DAPI+ areas. Figure 6A–D shows nuclei from Group III strains. The vegetative nucleus in Figure 6A is significantly smaller than the nuclei in other stages (Fig. 6B–D). The NOR are either peripheral and duplicated (Fig. 6B) or individual and central (Fig. 6C, D). Nuclear morphologies resembling those of zygote stages were also observed (Fig. 6D). While DAPI+ areas were sometimes present (arrows in Fig. 6C, D), they did not co-localize with ribosomal genes. Figure 6E–G shows Group IV nuclei, which also lack NOR-associated DAPI+ regions. A higher number of telomeric signals were detected in Group IV than Group III

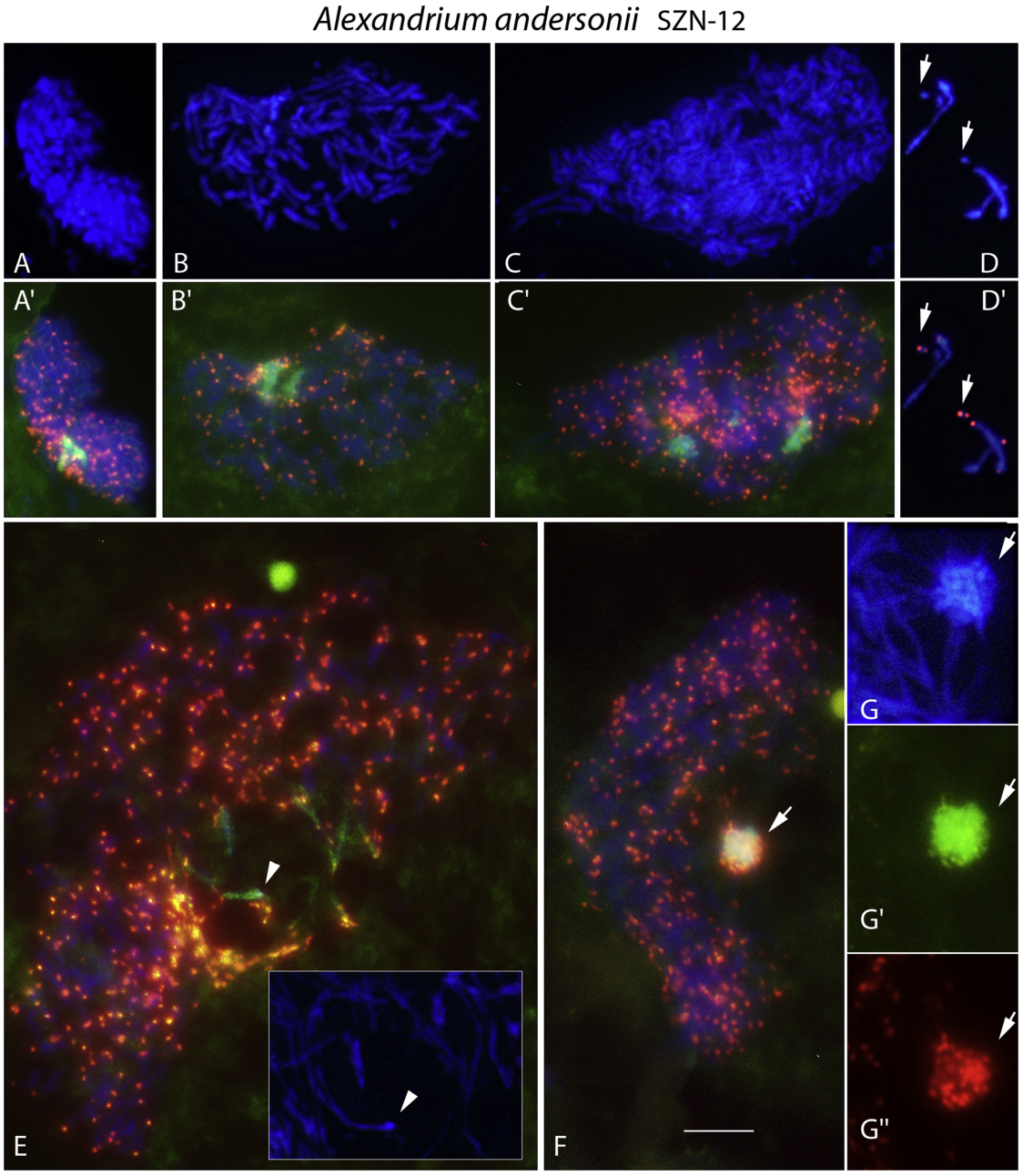

Figure 3. DNA DAPI staining (blue) and in situ hybridization of the digoxigenin-labeled pTa71 probe for the detection of ribosomal genes (green) and of the Dy547-labeled oligonucleotide $(CCCTAAA)_3$ for telomere localization (red) in *Alexandrium andersonii* SZN-12 cells. When not all probes are shown simultaneously, a single letter applies to photos in which only DAPI staining has been used and (‘) refers to the result with all probes. (**A**)Vegetative nuclei;(**B–C**) 2C stages; (**D**) detail of dot chromosomes with arrows pointing to the telomeres; (**E**) 2C stage as evidenced by the nuclear size and abundance of telomeres with disorganized nucleolus (arrow);(**F**) abundance of telomeres associated with the nucleolus (arrow) (see text for clarification); (**G, G′ and G″**) nucleolus detail, and with higher magnification, showing co-localization of DNA, rDNA and telomeric signals. Scale bars: 10 μm.

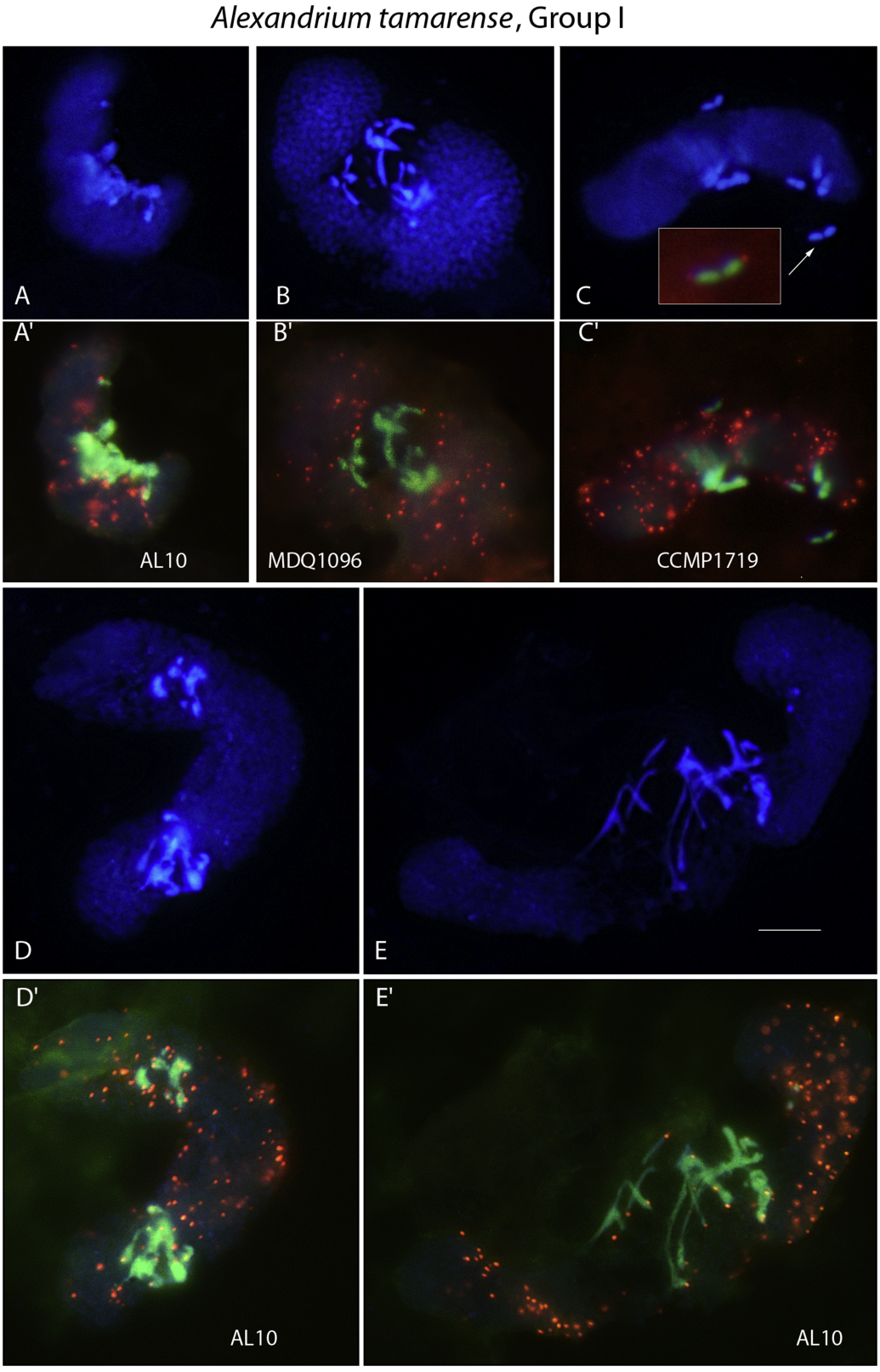
Alexandrium tamarense, Group I
A
B
C
A'
B'
C'
AL10
MDQ1096
CCMP1719
D
E
D'
E'
AL10
AL10

strains, but as in Group III they were not homogeneously distributed and were located mainly at the periphery of the nucleus.

Alexandrium affine and *Alexandrium margalefii*

In the species with the highest DNA content, *Alexandrium affine* (Fig. 7A, B) and *Alexandrium margalefii* (Fig. 7C), chromosomal differentiation was more difficult due to the higher level of nuclear compaction. However, labeling of the ribosomal genes demonstrated their central position. Several different nuclear morphologies were observed, including the notably smaller and more compact nuclei shown in Figure 7B. A larger nucleus containing a large number of ribosomal copies was seen in *A. margalefii*. Of the two species only in *A. margalefii* a DAPI+ signal was associated with ribosomal gene location (Fig. 7C).

We have summarized in Table 1 the previously described main differences in the NOR patterns between the studied species.

Phylogenetic Analyses

To discuss the above-described NOR patterns as a function of genetic distances between strains, we classified the studied clones based on their ITS regions (Table 2 and Fig. S1 in Supplementary Material). Strains of the *Alexandrium tamarense/catenella/fundyense* species complex formed a monophyletic clade that could be subdivided into four groups, Groups I (including genes A and B), II, III, and IV, all of which were strongly supported by bootstrap values of 100. Mean genetic distances (p) between groups in the species complex ranged from 0.079 to 0.181. The maximum intra-groups distance was 0.010, determined within Group IV.

Discussion

Dinoflagellates are eukaryotes with a very large number of seemingly identical and permanently condensed chromosomes. The genus *Alexandrium* includes species complexes comprising toxic and non-toxic ribotypes that share many morphological characters (Anderson et al. 2012) but which differ greatly in their genome sizes (LaJeunesse et al. 2005). These properties make this genus an interesting eukaryotic model to study the chromosomal location of ribosomal genes, since as shown by Prokopowich et al. (2003) in 162 species of plants and animals, their copy number is dependent on genome size. In other eukaryotic systems, rDNA organizational patterns are used to discriminate between species (see for examples in plants Adams et al. 2000; Leitch et al. 1992; She et al. 2012). Our results show that rRNA genes of *Alexandrium* are organized in chromosomal clusters, suggesting the existence of tandem arrays in NORs. Supporting our results, hybridization signals were not found outside the nucleolus. However, *Alexandrium* differs from other eukaryotes in that in some species these essential genes are carried on specialized chromosomes. This pattern of ribosomal gene organization was independent of genome size among species with relatively low DNA content but was consistently present among species with a high DNA content, even those not closely related. In the following, we first discuss about differences in chromosomal size and morphology in dinoflagellates based on our observations in the *Alexandrium* species examined in this work, as well as the use of NOR patterns as a tool for species identification and life cycle studies.

NOR Distribution Patterns

Low-DNA-content Species: *A. minutum* and *A. andersonii*

Only one prominent active nucleolus per cell was organized in all the *Alexandrium* species analyzed; however, the rDNA organizational patterns were quite different between species. In the metaphase chromosomes of *A. minutum*, ribosomal genes made up most of the bodies of some chromosomes, suggestive of chromosomal specialization with respect to the location of rRNA genes (Fig. 2E, insert). Some chromosomes featured constrictions in their centromeric regions and were thus more

Figure 4. DNA DAPI staining (blue) and in situ hybridization of the digoxigenin-labeled pTa71 probe for the detection of ribosomal genes (green) and of the Dy547-labeled oligonucleotide $(CCCTAAA)_3$ for telomere localization (red) in *Alexandrium* cells of Group I. When not all probes are shown simultaneously, a single letter applies to photos in which only DAPI staining has been used and (') refers to the result with all probes. (**A**, **C**) Vegetative nuclei;(**B**, **D**, **E**) 2C stages and putative zygotes. Note the chromosomal individualization in the inserts of (C) and in (E), with the locations of the telomeres and rDNA copies. The arrow in (C) shows a centromere-like constriction. Scale bars: 10 μm.

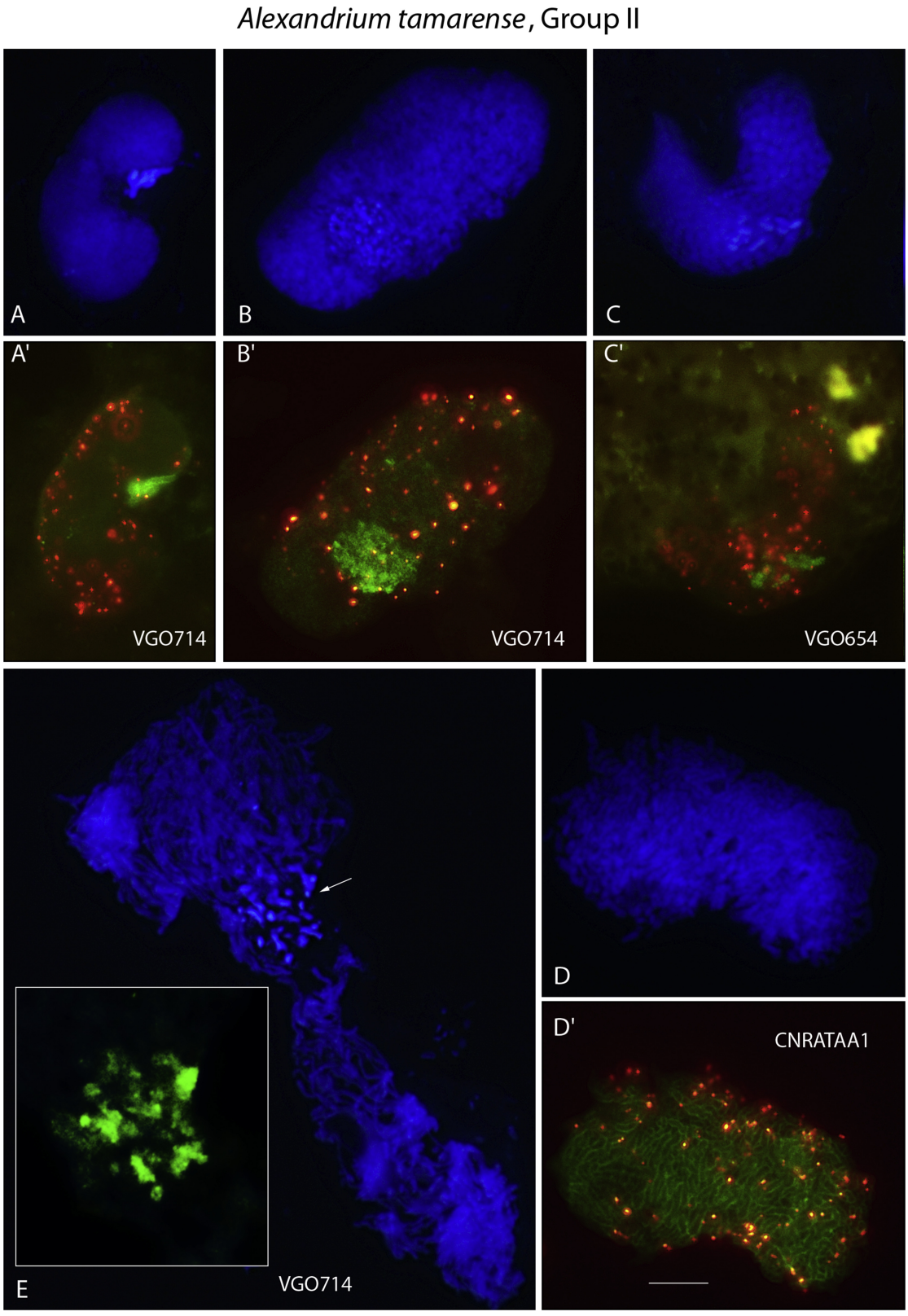
Alexandrium tamarense, Group II
A
B
C
A'
VGO714
B'
VGO714
C'
VGO654
D
D'
CNRATAA1
E
VGO714

Table 1. Main differences in the NOR patterns between the studied species.

Species	DAPI + chromosomes	Specialized ribosomal chromosomes	Distinct patterns between groups
A. andersonii	No	Yes	Telomere aggregation in *A. andersonii* nucleoli
A. minutum		No	
Group I	Yes	Yes	Group I has more rDNA repeats, and strains within the group are very similar in their rDNA organizational patterns.
Group II			Group II strains show comparatively fewer DAPI+ signals and rDNA repeats and greater pattern heterogeneity between strains. The rDNA organizational pattern of strain CNR-ATAA1 differed from the patterns of Groups I and II.
Group III	No. The few DAPI+ signals do not co-localize with the rDNA.	Yes	Group III shows significantly fewer telomeres and rDNA copies.
Group IV			
A. affine	No	?	High level of DNA compaction. *A. margalefii* nucleus is larger, with a higher rDNA copy number.
A. margalefii	Yes		

eukaryotic in their morphology than previously described. When chromosomal individualization was achieved (as seen in the metaphases D, E, and F of Fig. 2 and in Fig. 3D), the hybridization signals of the telomeric sequences were exclusively linked to chromosomal ends, and therefore, correspond to telomeres. We have generalized this result (i.e. telomeric sequences are specific to telomeres) to the rest of *Alexandrium* species in which chromosomal individualization was not possible. The *A. minutum* pattern of rRNA gene location was not seen in *A. andersonii*, despite its very similar genome size. Instead, in this species a very unusual pattern of nucleolus-associated telomere clustering was observed. An important feature of telomeres in normal interphase nuclei is that they do not overlap, nor do they form clusters or aggregates with other telomeres (Chuang et al. 2004). In contrast to the non-overlapping nature of telomeres in normal nuclei, telomeres of tumor nuclei tend to form aggregates (Mai and Garini 2006). Telomere-related proteins, however, are specifically associated with the nucleolus during DNA replication. For example, the ribonucleoprotein enzyme that adds telomeric nucleotide repeat sequences to the ends of chromosomes (telomerase reverse

Figure 5. DNA DAPI staining (blue) and in situ hybridization of the digoxigenin-labeled pTa71 probe for the detection of ribosomal genes (green) and of the Dy547-labeled oligonucleotide $(CCCTAAA)_3$ for telomere localization (red) in Group II cells. When not all probes are shown simultaneously, a single letter applies to photos in which only DAPI staining has been used and (') refers to the result with all probes. (**A**) A vegetative nucleus with its peripherally located NOR; (**B**) a clearly formed nucleolus;(**C**, **E**) the correlation between DAPI+ chromosomes and ribosomal genes, further highlighted by the arrow and detail in (E); (**D**) strain CNRATAA1, the only strain in the study that did not fit the pattern of Groups I and II. Scale bars: 10 μm.

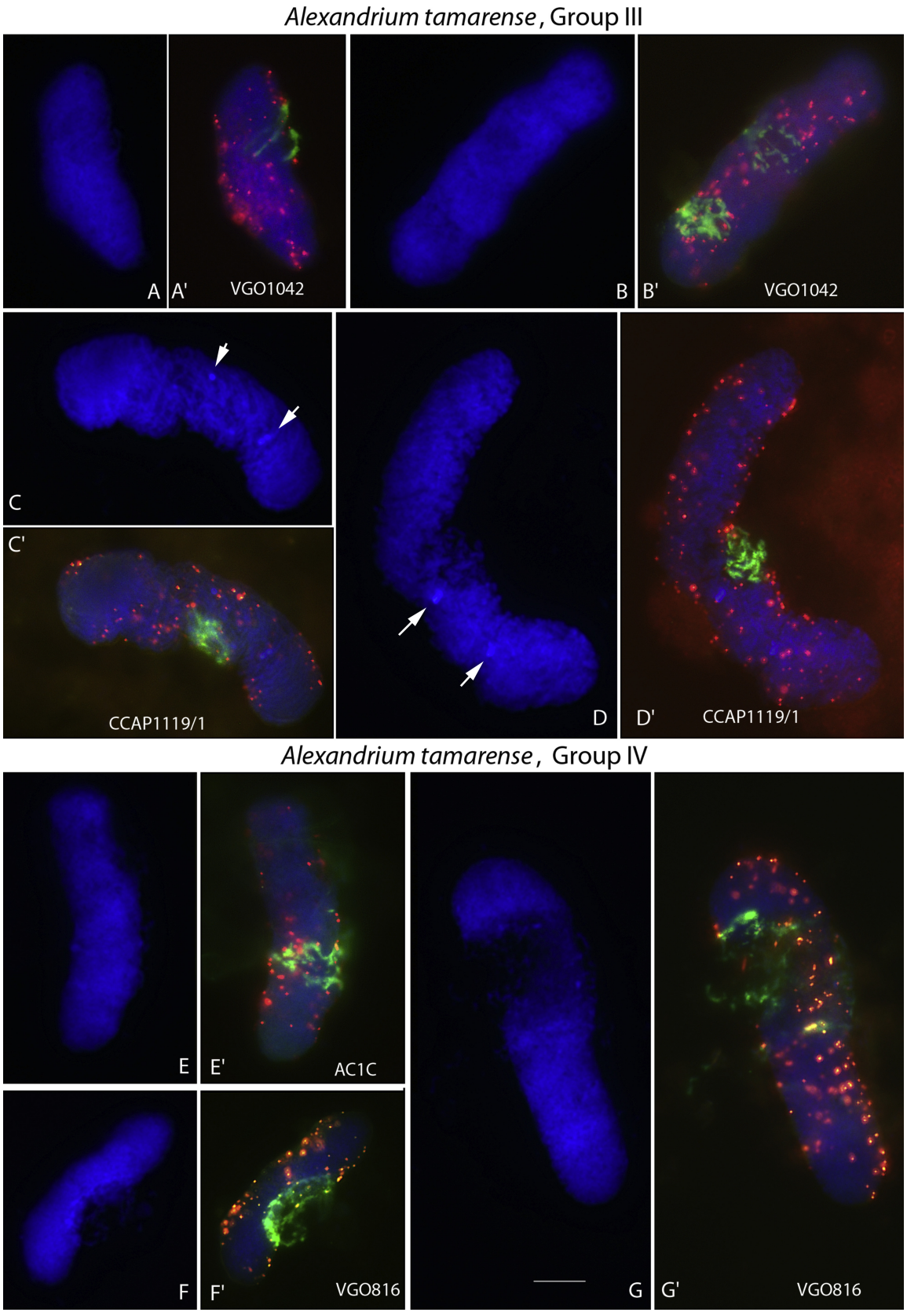
Alexandrium tamarense, Group III
A
A'
VGO1042
B
B'
VGO1042
C
C'
CCAP1119/1
D
D'
CCAP1119/1
Alexandrium tamarense, Group IV
E
E'
AC1C
F
F'
VGO816
G
G'
VGO816

transcriptase) remains sequestered in nucleoli until the telomeres are replicated, at late stages of S phase (Boisvert et al. 2007).The telomeric repeat binding factor 2 (which recognizes repeats at chromosomal ends) of humans also has a prominent nucleolar localization (Zhang et al. 2004). However, telomere aggregation in normal cells has only been observed in relation to the meiotic process, preceding meiotic chromosome synapsis in fission yeasts (Scherthan et al. 1994) and *Arabidopsis thaliana* (Armstrong et al. 2001). Whether the pattern observed in *A. andersonii* is sexually related is as yet unknown, but it seems to be a species-specific characteristic.

High-DNA-content Species: Specialized rDNA Chromosomes

Within and among strains of the *Alexandrium tamarense/catenella/fundyense* species complex there is a large variation in the characters traditionally used to differentiate species, such that genetic clades rather than biological species have been defined. We observed that a group of chromosomes in the Groups I–IV were mostly made up of ribosomal genes, a feature especially evident in Group I, which contained ribosomal genes in high copy numbers. In Groups I and II, the rDNA chromosomes were additionally characterized by a distinct and intense DAPI signature (DAPI+). DAPI staining is dependent on chromatin organization, binding strongly (+) to A/T rich sequences. To our knowledge, this is a novel eukaryotic organization of ribosomal genes. Other unusual rDNA organization patterns have been described in other eukaryotes. For example, in the slime molds *Physarum* and *Dictyostelium* and in the ciliated protozoans *Oxytricha Tetrahymena* and *Paramecium* rDNA is present extrachromosomally (Findly and Gall 1978 and references therein). *Physarum polycephalum* apparently lacks any chromosomal copies of rDNA, which instead forms linear extrachromosomal palindromes of a highly polymorphic nature based on minor sequence changes (Cockburn et al. 1978; Vogt and Braun 1976; Welker et al. 1985). In *Dictyostelium*, rDNA monomers associate as rings within interphase nuclei. These rings then disrupt to form linear aggregates of chromosome-sized clusters within the nuclei of cells arrested in mitosis (Parish et al. 1980; Sucgang et al. 2003). The rDNA clusters resemble true chromosomes—which has resulted in their misidentification as a seventh chromosome in this organism—and their formation may ensure the efficient segregation of rDNA during mitosis (Sucgang et al. 2003). A similar case could be made for the characteristic distribution of the ribosomal genes in the *Alexandrium tamarense/catenella/fundyense* species complex, but their chromosomal location is suggested by the location of telomeres at both extremes of the ribosomal array. This pattern should be verified by establishing that the number of "ribosomal chromosomes" is a species-specific landmark. We detected ribosomal genes either in heavily (Groups I and II) or lightly (Groups III and IV) DAPI-stained chromosomes, generally located in a central position with respect to the U-shaped nucleus.

Among the studied species in which we were able to clearly differentiate chromosomes and locate telomeres (and thus, confirm the position within true chromosomes of the rDNA copies), strains comprising the group I-V complex had the largest genomes. Confirmation of this large genome size would suggest that the NOR is related to genome size, although this pattern would need to be confirmed in other *Alexandrium* species with high DNA content. Genome size has molecular, biological, and ecological consequences. In dinoflagellates, their large genome may not correspond to a high gene diversity, as many gene copies may be duplications just slightly different from each other, similarly to what happened in the rRNA locus (Pellicer et al. 2010). Independently of this fact, the vital role played by ribosomal RNA (rRNA) makes it crucial to ensure the fast and correct transcription of the rDNA copies, which becomes more difficult as genome size increases because in eukaryotes, rDNA copy number and genome size are associated (Prokopowich et al. 2003). This association may be explained because extra rDNA copies facilitate detection of DNA damage

Figure 6. DNA DAPI staining (blue) and in situ hybridization of the digoxigenin-labeled pTa71 probe for the detection of ribosomal genes (green) and of the Dy547-labeled oligonucleotide $(CCCTAAA)_3$ for telomere localization (red) in Groups III and IV. When not all probes are shown simultaneously, a single letter applies to photos in which only DAPI staining has been used and (') refers to the result with all probes. The cells contain the specialized chromosomes but no DAPI+ areas; (**A–D**) Group III strains contain nuclei of different nuclear sizes, with the smallest corresponding to vegetative stages (A) and the largest to 2C stages which correspond to cells in 2G stage or zygotes (D). The same pattern was observed in *Alexandrium* Group IV (**E–G**). Note the fully formed nucleolus in (F) and the lack of DAPI+ areas in the nucleus in (G). Scale bars: 10 μm.

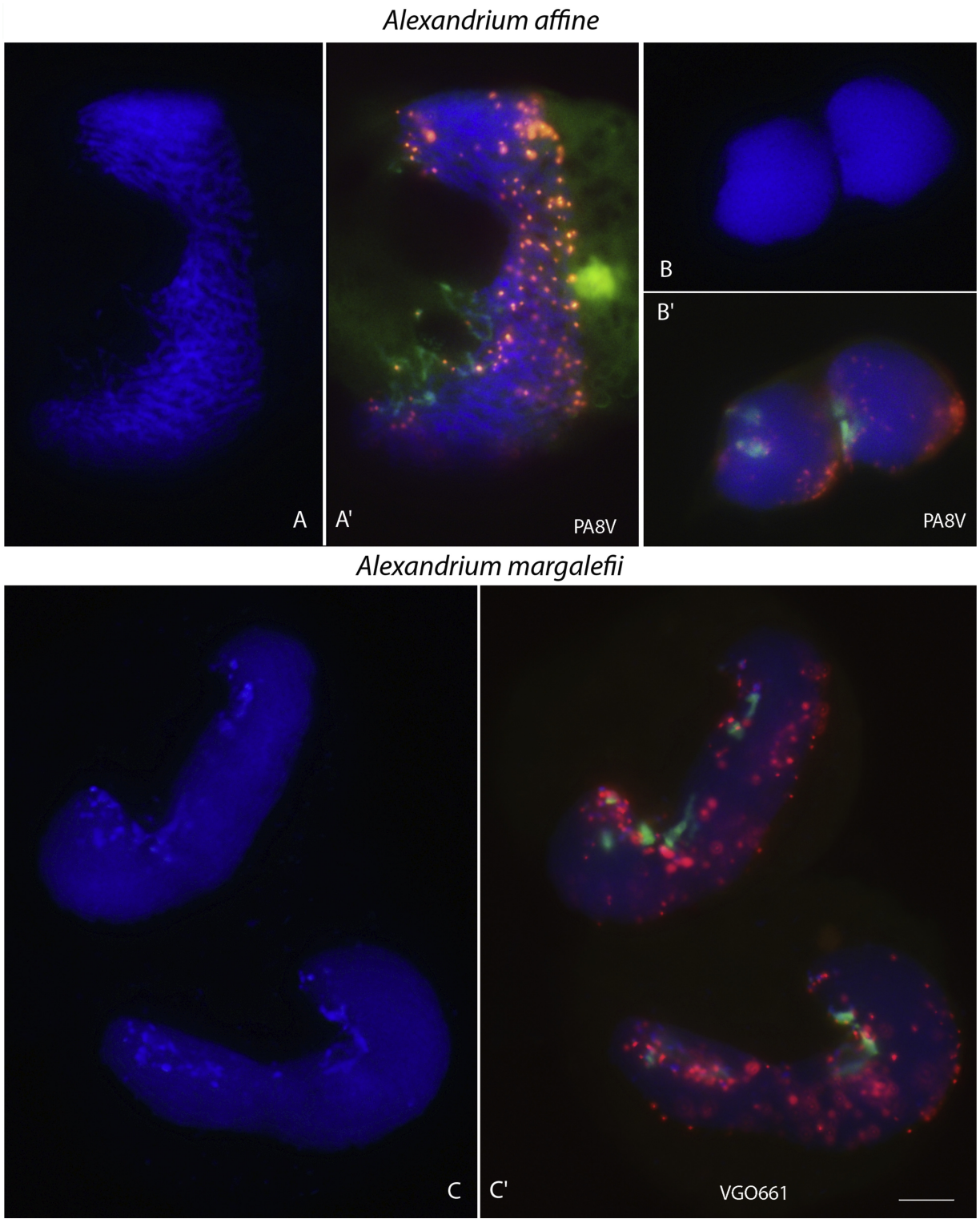

Figure 7. DNA DAPI staining (blue) and in situ hybridization of the digoxigenin-labeled pTa71 probe for the detection of ribosomal genes (green) and of the Dy547-labeled oligonucleotide $(CCCTAAA)_3$ for telomere localization (red) in *Alexandrium affine* (**A**, **B**)and *Alexandrium margalefii* (**C**). When not all probes are shown simultaneously, a single letter applies to photos in which only DAPI staining has been used and (') refers to the result with all probes. DAPI+ areas associated with the NOR were observed only in *A. margalefii*. Scale bars: 10 μm.

and repair by providing sufficient copies for ribosome biosynthesis. But their repetitive nature might be potentially dangerous in terms of genome stability, since in higher organisms abnormalities in rDNA transcription and the organization of the chromatin of the NOR have been related to aging and cancer (see, e.g., Kobayashi 2011 and references therein). Further and specific research needs to be done to validate or invalidate these suggested general eukaryotic theories in the complex dinoflagellate system. Similar to the suggested extrachromosomal palindrome encoding ribosomal RNA genes in *Dictyostelium* (Sucgang et al. 2003), the novel rDNA distribution in specialized ribosomal chromosomes reported here for some dinoflagellate species may offer a solution to the efficient transcription and segregation of the fundamental ribosomal genes during mitosis and meiosis.

NORs and the Evolutionary History of *Alexandrium*

Repeated DNA sequences have been suggested to play a major role in plant speciation (Bennett and Leitch 2005). In dinoflagellates, the arrangement of some tandemly repeated genes is complex and is not phylogenetically related. For example, both the length and sequence of the spliced leader (SL) RNA are conserved in all dinoflagellates, but the gene can be organized in single-gene tandem repeats or as mixed SL RNA-5S rRNA genes, without a phylogenetic trend in complexity (Zhang et al. 2009). The wide-ranging variability in the arrangements of 5S rRNA genes likely reflects the fact that they contain internal promoters, which are often transposed by diverse recombination mechanisms in species with short generation times and frequent founder effects (Drouin and Tsang 2012). However, this is not the case for the 45S genes, which are present at high copy number and are strongly expressed, such that both their sequence and their organization may reveal an evolutionary trend.

Alexandrium, although still under intense phylogenetic study, is a monophyletic lineage containing clearly differentiated species complexes (see review Anderson et al. 2012). From the studied species, the first cluster to diverge was that comprising *A. minutum and A. margalefii*, followed by the clusters containing *A. affine* and the *Alexandrium tamarense/catenella/fundyense* species complex (John et al. 2003; Orr et al. 2011; see also Fig. S1, Supplementary Material). According to John et al. (2003), divergence within this species complex can be explained as follows: a homogeneous *A. tamarense* population diverged in response to heterogeneous climatic and oceanographic conditions, forming Groups IV and III. Later, uplifting of the Panama Isthmus caused the divergence of Group I; finally, the drying up and subsequent filling of the Mediterranean Sea with subtropical water containing *A. tamarense* populations gave rise to Group II.

Our results show that the placement of the ribosomal genes changes within a genus, from the more conventional location in several chromosomes of *A. andersonii* to the chromosomal specialization of *A. minutum* and the *Alexandrium tamarense/catenella/fundyense* species complex. Because of the large differences in genome size between these two species, this characteristic is more evident in the I-V species complex. Consistent with their hypothetic origin, we found a more similar pattern in Groups I and II vs. Groups III and IV. Two rDNA gene variants in the group I were first reported by Scholin et al. (1994), as also determined in our phylogeny. Recently, Miranda et al. (2012) found in group I a much more complex genetic diversity based on a refined phylogeny using intragenomic SSU rDNA polymorphism. Nevertheless, this aspect was not included in our work, as strains from gene variant B were not analyzed in this study. Given the important difference in the number of repetitive rDNA regions between Groups I and II (fewer in Group II) and the clearly different NOR patterns in some cases, as shown in strain CNRATAA1 (Table 2), the possibility of a different rDNA organizational pattern between the A and B variants of Group I should be examined in further surveys. Ruling out a mistake, our molecular analyses confirmed the assignment of strain CNRATAA1within Group II (Fig. S1, Supplementary Material). The largest genetic distance was between Groups I and IV, whose members are sexually incompatible (Lilly et al. 2007). Similarly, Group I $\times$ Group III crosses yielded viable zygotes but no surviving offspring (Brosnahan et al. 2010). However, reproductive isolation has yet to be studied in the other clade combinations; thus, whether these groups correspond to different biological species remains unclear. Our results support a closer relation between Groups I and II, in which NOR clusters were associated with DAPI+ areas, and between Groups III and IV, in which this association was lacking. In addition, Group III strains contained fewer chromosomes than Group IV, although genome size was not significantly different within the I–IV assemblage. In fact, variability among strains within the I-IV group was significantly greater than determined in other species, highlighting the need to study more strains

Table 2. Characteristics of the dinoflagellate clonal strains employed in the study.

Species	Strain name	Isolation year	Origin	Clade	Genbank ribosomal sequence	FISH
A. minutum[1]	VGO650	2003	Brittany,(France)	-	KF018286, KF018287	Fig. 2 A-E
A. minutum[2]	VGO651	2003	Brittany,(France)		KF018284, KF018285	
A. minutum	AL1V (CCMP113)	1987	Vigo (Spain)	-	JF521634	Fig. 2F, G
A. andersonii	SZN-12	1980	Town Cove (USA)	-	AJ308523	Fig. 3
A. affine	PA8V	1999	La Línea de la Concepción (Spain)	-	AJ632095	Fig. 7A, B
A. margalefii	VGO661	2003	Ebro Delta (Spain)	-	AM237339	Fig. 7C
A. cf. *tamarense*	MDQ1096	1996	Mar de Plata (Argentina)	Group I	AM292306	Fig. 4B
A. catenella	AL10	-	Monterey Bay (USA)		KF042352	Fig. 4A, 4D, 4E
A. cf. *fundyense*	CCMP1719	2005	Portsmouth (USA)		JF521624, JF521642 KF646469	Fig. 4C
A. cf. *kutnerae*	VGO714	2003	Port of Vilanova (Spain)	Group II	AM238515	Fig. 5A, B
A. cf. *tamarense*	CNR-ATAA1	2000	Puglia (Southern Italy)		AJ491152, KC702847, KC702848	Fig. 5D
A. tamarense	VGO654	2002	Pagera (Spain)		AM238650	Fig. 5C
A. tamarense	VGO1042	2010	Ebro Delta, (Spain)	Group III	KF018283	Fig. 6A, B
A. tamarense	CCAP1119/1	1957	Tamar estuary (England)		KC702845, KC702846	Fig. 6C, D
A. cf. *catenella*	VGO816	2004	Crique L'Anglé (France)	Group IV	AJ968680	Fig. 6F, G
A. cf. *catenella*	AC1C	2002	Port of Barcelona (Spain)		AJ532911	Fig. 6E

[1]Plate 1', without a ventral pore. [2]Plate 1', with a ventral pore.

to verify this finding. Nonetheless, morphologically cryptic groups could be distinguished based on the FISH analysis of the NOR patterns. This identification is highly relevant because members of these four groups may co-occur in some areas and may include toxic and non-toxic representatives. In addition, pairs formed by Groups I (toxic)/III (non-toxic) and II (non-toxic)/ IV (toxic) may be impossible to distinguish solely on the basis of morphology.

The rDNA gene copies of *A. margalefii* were in a similar location as those of *Alexandrium tamarense/catenella/fundyense* species complex and in both species were associated with DAPI+ areas, which suggests a similar chromosomal distribution, even though *A. affine* is phylogenetically closer to *A. margalefii* (Fig. S1, Supplementary Material). However, chromosomal individualization failed to fully localize the positions of the telomeres in *A. margalefii* and *A. affine*, the species with the highest DNA content. Therefore, the existence of ribosomal chromosomes remains to be determined in future research.

Life Cycle Studies

By combining nuclear and NOR shapes and sizes in cultures of sexual and asexual *Alexandrium minutum*, we were able to discriminate zygotes from vegetative stages. Some of the studied clones formed zygotes and hence can be considered homothallic (self-fertilizing), although they were originally identified as heterothallic (non-self-fertilizing), based on the failure to produce resting cysts. However, we did not systematically study sexual and asexual stage development, and therefore, our FISH-based life cycle characterization was not completely unambiguous. For example, some stages of division can be still misidentified as zygotes and vice versa. Stages in division are not expected to show duplicated NORs until two nuclei are clearly distinguished, as we observed nucleolar disorganization during metaphases. However, the squash preparations made for FISH make it difficult in occasions to clearly verify this aspect. However, NOR location offers additional and new information about the cell cycle stage, highly needed in life cycle studies in this group of organisms, which are characterized by a complex sexual cycle and by morphological similarities between sexual and vegetative stages.

Chromosomal Morphology

Unlike other eukaryotes, the chromosomes of dinoflagellates are permanently condensed and undifferentiated (Rizzo 1991; Soyer-Gobillard et al. 1996, 1999). To our knowledge, neither their shapes nor their morphological distinctions have been previously analyzed. In this study, we found differences in nuclear morphology and the state of chromatin condensation during both the cell cycle and different life cycle stages, as well as differences in chromosomal size and morphology. We also identified dot chromosomes and chromosomal constrictions, some associated with the NOR and resembling eukaryotic centromeres. Ordinary centromeres are not a feature of dinoflagellate chromosomes, which during mitosis attach to the nuclear membrane rather than to the spindle (Kubai and Ris 1969). However, whether these constrictions are not only morphologically but also functionally related to a conventional centromere, and specifically to typical metacentric chromosomes, remains to be determined.

Conclusions

The present work provides evidence for rDNA cluster polymorphisms between morphologically undifferentiated species and describes important novel features of the dinoflagellate nucleus. Our results support the conclusion that dinoflagellate chromosomes are more “eukaryotic” than previously thought, as they differ in size (including dot chromosomes) and contain eukaryotic constrictions reminiscent of centromeres as well as discrete NORs and specialized NOR-bearing chromosomes. Chromosomes that almost exclusively carry rDNA genes are, to our knowledge, a novel finding within eukaryotes and might be an adaptation to accommodate the large number of rDNA copies in the accordingly very large genome of dinoflagellates, although it was not seen in the species with the smallest genome analyzed. Additionally, we were able to use NOR patterns to resolve cryptic species and to identify some sexual life cycle stages. However, further studies are needed to understand the processes responsible for the differences in NOR structure and how NOR polymorphism relates to differences in the regulation of rRNA gene activity in the studied species.

Methods

Dinoflagellate strains: The strains employed in this study are listed in Table 2. All strains are regularly maintained at the Centro Oceanográfico de Vigo (CCVIEO; the Culture Collection of Harmful Microalgae of the Spanish Institute of Oceanography), where they are available upon request.

Culture conditions: The strains were cultured at 20 °C with an irradiance of approx. 90 μmol photons $m^{-2}s^{-1}$ and a photoperiod of 12:12 h L:D (light:dark). Culture stocks were maintained in Iwaki 50-mL flasks filled with 30 mL of L1 medium (Guillard and Hargraves 1993) without added silica. The medium was prepared using Atlantic seawater adjusted to a salinity of 30 psu by the addition of sterile distilled water. Additionally, cultures were sexually induced by nutrient limitation using medium without added nitrates or phosphates. Among the studied species, only *A. minutum* is heterothallic, i.e., two different compatible strains must be crossed to induce sexuality and resting cyst formation (Figueroa et al. 2007). The sexual cycle of the other species has not been well studied, but in many cases homothally (self-fertility) has been reported (see revision of (Anderson et al. 2012). *A. minutum* duplicate out-crosses using the strains VGO650 and VGO651 (following the sexual compatibility results of (Figueroa et al. 2007, 2011)) were conducted in sterile polystyrene Petri dishes (Iwaki, Japan, 16-mm diameter) containing either 10 mL of L1 medium without added phosphate (L1-P) or L1 medium without added nitrate (L1-N). The dishes were inoculated with exponentially growing cells (2000–4000 cells mL^{-1}) to a final concentration of 300 cells mL^{-1} (150 cells mL^{-1} from each compatible strain). For the other species, only self-crosses of clonal strains were performed, using the same methodology.

Flow cytometry: Exponentially growing cultures of *Alexandrium* were incubated for 48 h in darkness to synchronize cell division (Figueroa et al. 2010; Taroncher-Oldenburg et al. 1997). Fifty mL of culture was filtered through a 5.0-μm pore size membrane filter (Millipore, Ireland), fixed with 1% paraformaldehyde for 10 min, and washed in PBS (pH 7, Sigma-Aldrich, St. Louis, USA) with centrifugation at 1200 *g* × 10 min. The pellet was resuspended in 2 mL of cold methanol and stored for at least 12 h at 4 °C to achieve chlorophyll extraction. The cells were then again washed twice in PBS and the pellet was resuspended in staining solution (PBS, 0.1 mg propidium iodide mL^{-1} and 2 μg RNaseA mL^{-1}) for at least 2 h before analysis. A Beckman FC500 bench model flow cytometer with a laser emitting at 488 nm was used. Triplicate samples were run at low speed (approx. 18 μL min^{-1}) and data were acquired in linear and log modes until at least 1000 events had been recorded. As DNA standard, 10 μL of a triploid DNA trout solution (7.8 pg DNA/nucleus, Biosure, USA) was added to each sample. The fluorescence emission of propidium iodide was detected at 620 nm. FlowJo 7.6 (Tree Star, Inc. USA) was used to compute peak numbers, coefficients of variation (CVs), and peak ratios for the DNA fluorescence distributions in a population. CVs above 10 were discarded from the analyses.

Fluorescence in situ hybridization (FISH): *Slide preparation*. Cells were harvested by gentle centrifugation at 1200 *g*, treated with Liquinox following (Adamich and Sweeney 1976), and fixed in ethanol:acetic acid 3:1 (v/v) for at least 24 h. The fixed cells were then squashed onto clean microscope slides in a drop of 45% acetic acid. The slides were frozen to remove the cover and air-dried. *DNA probes.* The DNA probe used for mapping the rDNA genes was pTa71. This plasmid contains a 9-kb *Eco*RI fragment from *Triticum aestivum* that includes the 18S-5.8S-26S rDNA region and intergenic spacers (Gerlach and Bedbrook 1979). pTa71 was labeled with digoxigenin-11-dUTP using a kit from Roche (Dig-Nick translation mix). Telomeres were detected using the deoxyribonucleotide oligomer probe (5′-CCCTAAA-3′)$_3$, synthesized with Dy547 (red), at both ends (Isogen Life Science). *Procedure*. Cell preparations (at least two replicates per strain and hundreds of cells per preparation) were incubated with DNase-free RNase A, post-fixed in freshly depolymerized 4% (w/v) paraformaldehyde, dehydrated in a graded ethanol series, and air-dried as described in Alverca et al. (2007). The cell samples were then denatured by placing the slides in an incubator at 75 °C for 7 min, with the temperature controlled using a programmable thermal controller (PT-100, M.J. Research Inc.) Hybridization was carried out by the addition of 30 μL of hybridization mixture (50% deionized formamide, 10% dextran sulfate, 2× SSC, and 0.33% SDS) containing 100 ng of the digoxigenated pTa71 probe and 2 pmol of the directly labeled telomeric oligonucleotide probe to each slide preparation, followed by incubation at 37 °C usually overnight. Post-hybridization washes of the slides were done in Coplin jars for 10 min with 4× SSC/Tween20 at room temperature. The digoxigenin-labeled ribosomal probe was detected by incubating the slides in fluoresceinated anti-digoxigenin (Roche Applied Science) in 5% (w/v) BSA for 1 h at 37 °C. No immunocytochemical procedures were required for the detection of the Dy-547 telomeric probe. The slides were rinsed for 10 min in 4× SSC/Tween20, DNA-stained with DAPI, and mounted in antifade solution (Vector Laboratories). Microscopic analyses were conducted using an epifluorescence Axiophot Zeiss system. Images were captured with a cooled CCD camera Nikon DS and merged using Adobe Photoshop. The images were optimized for best contrast and brightness using the same program but only those functions that treated all pixels in the image equally.

Molecular analyses: *DNA extraction*. *Alexandrium* strains (1 mL of actively growing cultures) were centrifuged 2 min at 11,400 *g* using a table top minicentrifuge (Eppendorf). DNA extracts (30 μL) were prepared following a Chelex extraction procedure previously described in Litaker et al. (2010). The samples were quantified on a Nanodrop Lite spectrophotometer (Thermo Fisher Scientific Inc., Waltham, MA, USA) and immediately used for PCR amplification. *PCR amplification and DNA sequencing*. The ITS regions and partial LSUrDNA (D1-D3 domains) were amplified using the primer pairs ITSF01/LSUB (5′-GAGGAAGGAGAAGTCGTAACAAGG-3′/5′-ACGAACGATTTGCACGTCAG-3′)(Ki and Han 2007; Scholin et al. 1994) to produce readable sequences of 1417–1475 bases (with the exception of *A.minutum* AL10, for which a 670-base fragment was obtained). The amplification reaction mixtures (25 μL) contained 2 mM $MgCl_2$, 0.25 pmol of each primer, 0.2 mM of dNTPs, 0.65 units Taq DNA polymerase (Qiagen, California, USA), and 2 μL of the DNA Chelex extracts. The DNA was amplified in a SureCycler 8800 thermal cycler (Agilent Technologies Inc., Santa Clara, CA, USA) under the following conditions: denaturation for 10 min 94 °C followed by 40 cycles of denaturation for 1 min at 94 °C, 1 min of annealing at 57 °C, a 1-min extension at 72 °C, and a final 10-min extension at 72 °C. A 10-μL aliquot of each PCR was checked by agarose gel electrophoresis (1% TAE, 70 V) and GelRed DNA gel staining (Biotium Inc., Hayward, CA, USA). PCR products were cloned using the Strata Clone PCR cloning kit (Agilent) following the manufacturer's specifications. Plasmid DNA was purified using ExoSAP-IT (USB Corporation, Cleveland, Ohio, USA) and then sequenced using the Big Dye Terminator v3.1 reaction cycle sequencing kit (Applied Biosystems, Foster City, CA, USA) and the AB 3130 sequencer (Applied Biosystems) at the CACTI sequencing facilities (Universidade de Vigo, Spain). The amplified sequences obtained were deposited in GenBank (accession numbers are listed in Table 2).

Phylogenetic analyses: The amplified sequences were aligned using CLUSTALW multiple alignment in Geneious®Pro 5.6.6 using default parameters (Cost matrix: IUB, gap open cost:15, gap extend cost:6.6). Subsequently, only ITS-1, 5.8SrDNA and ITS-2 sequences were selected to elaborate the phylogenetic trees (515 bases, final alignment).

Poorly aligned positions and divergent regions were checked using the Gblocks software (Castresana 2000). Finally, 333 bases (65% of the original ITS alignment) were saved by Gblocks. The phylogenetic relationships were determined using MrBayes v3.1(Huelsenbeck and Ronquist 2001). A general time reversible model (GTR, submodel 112312) was selected when sampling the substitution model (program parameters state freqpr = dirichlet (1,1,1,1), nst = mixed, rates =gamma, nswaps = 1). The phylogenetic analyses involved two parallel analyses, each with four chains. Starting trees for each chain were selected randomly using the default values for the MrBayes program. There were 173 unique site patterns. The analysis was based on 100,000 generations and final split frequencies were less than 0.05. Posterior probabilities were calculated from every 100th tree, sampled after log-likelihood stabilization ("burn-in" phase). For comparative purposes, ML phylogenetic analyses were also conducted after different models of DNA substitution, and the associated parameters were estimated using Modeltest 3.7(Posada and Crandall 1998). The ML phylogeny was performed in PhyML 3.0 (Guindon et al. 2010) using a K80 with a γ distribution (K80 + G) model, on the South of France bioinformatics platform (http://www.atgc-montpellier.fr/phyml). Bootstrap values were estimated from 1,000 replicates. The overall topologies obtained with the ML and Bayesian inference methods were very similar. The phylogenetic tree was represented using the Bayesian inference with posterior probability and bootstrap values from the ML method. Groups I to IV of the "*A. tamarense/catenella/fundyense* species complex" indicated in our phylogeny match the groups previously designated by Lilly et al (2007) using large subunit (LSU) rRNA genes. Several strains assigned to Groups I to IV by these authors were included in our phylogenetic analyses to confirm the coherence of our grouping.

Acknowledgements

The present work was funded by a FORMAS (Sweden) project to R. I. Figueroa. We thank Marie Svensson for technical help.

Appendix A. Supplementary Data

Supplementary data associated with this article can be found, in the online version, at http://dx.doi.org/10.1016/j.protis.2014.04.001.

References

Adamich M, Sweeney BM (1976) The preparation and characterization of *Gonyaulax* spheroplasts. Planta (Berl) **130**:1–6

Adams SP, Leitch IJ, Bennett MD, Chase MW, Leitch AR (2000) Ribosomal DNA evolution and phylogeny in *Aloe* (Asphodelaceae). Am J Bot **87**:1578–1583

Alverca E, Cuadrado A, Jouve N, Franca S, Moreno Díaz de la Espina S (2007) Telomeric DNA localization on dinoflagellate chromosomes: structural and evolutionary implications. Cytogenet Genome Res **116**:224–231

Anderson DM, Cembella AD, Hallegraeff GM (eds) Physiological Ecology of Harmful Algal Blooms. NATO ASI Series. Series G, Ecological Sciences. Springer-Verlag, Bermuda, 662 p

Anderson DM, Alpermann TJ, Cembella AD, Collos Y, Masseret E, Montresor M (2012) The globally distributed genus *Alexandrium*: Multifaceted roles in marine ecosystems and impacts on human health. Harmful Algae **14**:10–35, http://dx.doi.org/10.1016/j.hal.2011.10.012

Armstrong SJ, Franklin FC, Jones GH (2001) Nucleolus-associated telomere clustering and pairing precede meiotic chromosome synapsis in *Arabidopsis thaliana*. J Cell Sci **114**:4207–4217

Bennett MD, Leitch IJ (2005) Genome Size Evolution in Plants. In Gregory TR (ed) The Evolution of the Genome. Elsevier, San Diego, pp 89–151

Boisvert FM, van Koningsbruggen S, Navascués J, Lamond AI (2007) The multifunctional nucleolus. Nat Rev Mol Cell Biol **8**:574–585

Britton-Davidian J, Cazaux B, Catalan J (2012) Chromosomal dynamics of nucleolar organizer regions (NORs) in the house mouse: micro-evolutionary insights. Heredity (Edinb) **108**:68–74, http://dx.doi.org/10.1038/hdy.2011.105

Brosnahan ML, Kulis DM, Solow AR, Erdner D, Percy L, Lewis J, Anderson DM (2010) Outbreeding lethality between toxic Group I and nontoxic Group III *Alexandrium tamarense* spp. isolates: Predominance of heterotypic encystment and implications for mating interactions and biogeography. Deep-Sea Res PT II: **57**:175-189 http://dx.doi.org/10.1016/j.dsr2.2009.09.005

Carvalho ANA, Guedes-Pinto H, Lima-Brito J (2011) Physical localization of NORs and ITS length variants in old Portuguese durum wheat cultivars. J Genet **90**:95–101

Castresana J (2000) Selection of conserved blocks from multiple alignments for their use in phylogenetic analysis. Mol Biol Evol **17**:540–552

Chakraborty A, Kenmochi N (2012) Ribosomes and Ribosomal Proteins: More Than Just 'Housekeeping'. eLS http://dx.doi.org/10.1002/9780470015902.a0005055.pub2

Chow M, Yan K, Bennett M, Wong J (2010) Birefringence and DNA condensation of liquid crystalline chromosomes. Eukaryot Cell **9**:1577–1587, http://dx.doi.org/10.1128/EC.00026-10

Chuang TC, Moshir S, Garini Y, Chuang AY, Young IT, Vermolen B, van den Doel R, Mougey V, Perrin M, Braun M, Kerr PD, Fest T, Boukamp P, Mai S (2004) The three-dimensional organization of telomeres in the nucleus of mammalian cells. BMC Biology **2**:12, http://dx.doi.org/10.1186/1741-7007-2-12

Cockburn AF, Taylor WC, Firtel RA (1978) *Dictyostelium* rDNA consists of non-chromosomal palindromic dimers containing 5S and 36S coding regions. Chromosoma **70**: 19–29

Drouin G, Tsang C (2012) 5S rRNA gene arrangements in protists: a case of nonadaptive evolution. J Mol Evol **74**:342–351, http://dx.doi.org/10.1007/s00239-012-9512-5

Figueroa R, Bravo I, Garcés E (2006) Multiple routes of sexuality in *Alexandrium taylori* (Dinophyceae)

in culture. J Phycol **42**:1028–1039, http://dx.doi.org/10.1111/j.1529-8817.2006.00262.x

Figueroa RI, Garcés E, Bravo I (2007) Comparative study of the life cycles of *Alexandrium tamutum* and *Alexandrium minutum* (Gonyaulacales, Dinophyceae) in culture. J Phycol **43**:1039–1053, http://dx.doi.org/10.1111/j.1529-8817.2007.00393.x

Figueroa RI, Garcés E, Bravo I (2010) The use of flow cytometry for species identification and life-cycle studies in dinoflagellates. Deep-Sea Res PT II **57**:301–307, http://dx.doi.org/10.1016/j.dsr2.2009.09.008

Figueroa R, Vázquez J, Massanet A, Murado M, Bravo I (2011) Interactive effects of salinity and temperature on planozygote and cyst formation of *Alexandrium minutum* (Dinophyceae) in culture. J Phycol **47**:13–24, http://dx.doi.org/10.1111/j.1529-8817.2010.00937.x

Findly RC, Gall JG (1978) Free ribosomal RNA genes in *Paramecium* are tandemly repeated. Proc Natl Acad Sci USA **75**:3312–3316

Fojtová M, Wong JT, Dvorácková M, Yan KT, Sýkorová E, Fajkus J (2010) Telomere maintenance in liquid crystalline chromosomes of dinoflagellates. Chromosoma **119**:485–493, http://dx.doi.org/10.1007/s00412-010-0272-y

Frolov SV, Frolova VN (2004) Karyological differentiation of northern Dolly Varden and sympatric chars of the genus *Salvelinus* in northeastern Russia. Environ Biol Fish **69**:441–447

Gerlach WL, Bedbrook JR (1979) Cloning and characterization of ribosomal RNA genes from wheat and barley. Nucleic Acids Res **7**:1869–1885

Guillard RRL, Hargraves PE (1993) *Stichochrysis immobilis* is a diatom, not a chrysophyte. Phycologia **32**:234–236, http://dx.doi.org/10.2216/i0031-8884-32-3-234.1

Guindon S, Dufayard JF, Lefort V, Anisimova M, Hordijk W, Gascuel O (2010) New algorithms and methods to estimate maximum-likelihood phylogenies: assessing the performance of PhyML 3.0. Syst Biol **59**:307–321, http://dx.doi.org/10.1093/sysbio/syq010

Hackett JD, Anderson DM, Erdner D, Bhattacharya D (2004) Dinoflagellates: a remarkable evolutionary experiment. Am J Bot **91**, http://dx.doi.org/10.3732/ajb.91.10.1523, 1523-1515-1534

Hillis DM, Dixon MT (1991) Ribosomal DNA: molecular evolution and phylogenetic inference. Q J Florida Acad Sci **66**:411–453

Hou Y, Lin S (2009) Distinct gene number-genome size relationships for eukaryotes and non-eukaryotes: gene content estimation for dinoflaellate genomes. PloS One **4(9)**:e6978, http://dx.doi.org/10.1371/journal.pone.0006978

Huelsenbeck JP, Ronquist F (2001) MRBAYES: Bayesian inference of phylogenetic trees. Bioinformatics **17**:754–755

Jaeckisch N, Yang I, Wohlrab S, Glöckner G, Kroymann J, Vogel H, Cembella A, John U (2011) Comparative genomic and transcriptomic characterization of the toxigenic marine dinoflagellate *Alexandrium ostenfeldii*. PloS One **6(12)**:e28012, http://dx.doi.org/10.1371/journal.pone.0028012

John U, Fensome RA, Medlin LK (2003) The application of a molecular clock based on molecular sequences and the fossil record to explain biogeographic distributions within de *Alexandrium tamarense* "species complex" (Dinophyceae). Mol Biol Evol **20**:1015–1027

Kellenberger E (1988) About the organization of condensed and decondensed non-eukaryotic DNA and the concept of vegetative DNA (a critical review). Biophys Chem **29**:51–62

Ki J-S, Han M-S (2007) Rapid molecular identification of the harmful freshwater dinoflagellate *Peridinium* in various life stages using genus-specific single-cell PCR. J Appl Phycol **19**:467–470, http://dx.doi.org/10.1007/s10811-007-9157-8

Kobayashi T (2011) Regulation of ribosomal RNA gene copy number and its role in modulating genome integrity and evolutionary adaptability in yeast. Cell Mol Life Sci **68**:1395–1403, http://dx.doi.org/10.1007/s00018-010-0613-2

Kubai DF, Ris H (1969) Division in the dinoflagellate *Gyrodinium cohnii* (Schiller). A new type of nuclear reproduction. J Cell Biol **40**:508–528

LaJeunesse TC, Lambert G, Andersen RA, Coffroth MA, Galbraith DW (2005) *Symbiodinium* (Pyrrhophyta) genome sizes (DNA content) are smallest among dinoflagellates. J Phycol **41**:880–886, http://dx.doi.org/10.1111/j.1529-8817.2005.00111.x

Leitch AR, Mosgoller W, Shi M, Heslop-Harrison JS (1992) Different patterns of rDNA organization at interphase in nuclei of wheat and rye. J Cell Sci **101**:751–757

Lilly EL, Halanych KM, Anderson DM (2007) Species boundaries and global biogeography of the *Alexandrium tamarense* complex (Dinophyceae). J Phycol **43**:1329–1338, http://dx.doi.org/10.1111/j.1529-8817.2007.00420.x

Lin S (2011) Genomic understanding of dinoflagellates. Res Microbiol **162**:551–569, http://dx.doi.org/10.1016/j.resmic.2011.04.006

Lin S, Zhuang H, Tran B, Gill J (2010) Spliced leader-based metatranscriptomic analyses lead to recognition of hidden genomic features in dinoflagellates. Proc Natl Acad Sci USA **107**:20033–20038, http://dx.doi.org/10.1073/pnas.1007246107

Litaker RW, Vandersea MW, Faust MA, Kibler SR, Nau AW, Holland WC, Chinain M, Holmes MJ, Tester PA (2010) Global distribution of ciguatera causing dinoflagellates in the genus *Gambierdiscus*. Toxicon **56**:711–730, http://dx.doi.org/10.1016/j.toxicon.2010.05.017

Mai S, Garini Y (2006) The significance of telomeric aggregates in the interphase nuclei of tumor cells. J Cell Biochem **97**:904–915

Miranda LN, Zhuang Y, Zhang H, Lin S (2012) Phylogenetic analysis guided by intragenomic SSU rDNA polymorphism refines classification of *Alexandrium tamarense* species complex. Harmful Algae **16**:35–48, http://dx.doi.org/10.1016/j.hal.2012.01.002

Moreau H, Geraud ML, Bhaud Y, Soyer-Gobillard MO (1998) Cloning, characterization and chromosomal localization of a repeated sequence in *Crypthecodinium cohnii*, a marine dinoflagellate. Int Microbiol **1**:35–43

Okamoto N, Horák A, Keeling PJ (2012) Description of two species of early branching dinoflagellates, *Psammosa pacifica* n. g., n. sp. and *P. atlantica* n. sp. PLoS One **7(6)**:e34900, http://dx.doi.org/10.1371/journal.pone.0034900

Orr RJS, Stuken A, Rundberget T, Eikrem W, Jakobsen KS (2011) Improved phylogenetic resolution of toxic and non-toxic *Alexandrium* strains using a concatenated rDNA approach. Harmful Algae **10**:676–688, http://dx.doi.org/10.1016/j.hal.2011.05.003

Parish RW, Schmidlin S, Fuhrer S, Widmer R (1980) Electrophoretic isolation of nucleosomes from *Dictyostelium* nuclei and nucleoli: proteins associated with monomers and dimers. FEBS Lett **110**:236–240

Pawlowski J, Audic S, Adl S, Bass D, Belbahri L, Berney C, Bowser SS, Cepicka I, Decelle J, Dunthorn M, Fiore-Donno AM, Gile GH, Holzmann M, Jahn R, Jirku M, Keeling PJ, Kostka M, Kudryavtsev A, Lara E, Lukes J, Mann DG, Mitchell EAD, Nitsche F, Romeralo M, Saunders GW, Simpson AGB, Smirnov AV, Spouge JL, Stern RF, Stoeck T, Zimmermann J, Schindel D, de Vargas C (2012) CBOL Protist Working Group: Barcoding eukaryotic richness beyond the animal, plant, and fungal kingdoms. PLoS Biol **10**:e1001419, http://dx.doi.org/10.1371/journal.pbio.1001419

Pellicer J, Fay MF, Leitch IJ (2010) The largest eukaryotic genome of them all? Bot J Linn Soc **164**:10–15, http://dx.doi.org/10.1111/j.1095-8339.2010.01072.x

Pfiester LA, Anderson DM (1987) Dinoflagellate Reproduction. In Taylor FJR (ed) The Biology of Dinoflagellates. Bot Monogr Vol 21. Blackwell Sci Publ, Oxford, pp 611–648

Posada D, Crandall K (1998) MODELTEST: testing the model of DNA substitution. Bioinformatics **14**:817–818

Prokopowich CD, Gregory TR, Crease TJ (2003) The correlation between rDNA copy number and genome size in eukaryotes. Genome **46**:48–50, http://dx.doi.org/10.1139/G02-103

Reinaldo Cruz Campos J, Ananias F, Aguirre Brasileiro C, Yamamoto M, Fernando Baptista Haddad C, Kasahara S (2009) Chromosome evolution in three Brazilian *Leptodactylus* species (Anura, Leptodactylidae), with phylogenetic considerations. Hereditas **146**:104–111, http://dx.doi.org/10.1111/j.1601-5223.2009.02100.x

Rill RL, Livolant F, Aldrich HC, Davidson MW (1989) Electron-microscopy of liquid-crystalline DNA - direct evidence for cholesteric-like organization of DNA in dinoflagellate chromosomes. Chromosoma **98**:280–286

Rizzo PJ (1991) The enigma of the dinoflagellate chromosome. JProtozool **38**:246–252, http://dx.doi.org/10.1111/j.1550-7408.1991.tb04437.x

Roy S, Morse D (2012) A full suite of histone and histone modifying genes are transcribed in the dinoflagellate *Lingulodinium*. PLoS One **7(4)**:e34340, http://dx.doi.org/10.1371/journal.pone.0034340

Scherthan H, Bähler J, Kohli J (1994) Dynamics of chromosome organization and pairing during meiotic prophase in fission yeast. J Cell Biol **127**:273–285

Scholin CA, Herzog M, Sogin M, Anderson DM (1994) Identification of group and strain specific genetic markers for globally distributed *Alexandrium* (Dinophyceae). II. Sequence analysis of a fragment of the LSU rRNA gene. J Phycol **30**:999–1011, http://dx.doi.org/10.1111/j.0022-3646.1994.00999.x

She C-W, Jiang X-H, Song Y-C (2012) Comparison of the organization pattern of the rRNA gene in plants using fluorescence in situ hybridization. Plant Sci J **30**:169–177, http://dx.doi.org/10.3724/SP.J.1142.2012.20169

Soyer-Gobillard MO, Ausseil J, Geraud ML (1996) Nuclear and cytoplasmic actin in dinoflagellates. Biol Cell **87**:17–35

Soyer-Gobillard MO, Gillet B, Géraud M-L, Bhaud Y (1999) Dinoflagellate chromosome behaviour during stages of replication. Int Microbiol **2**:93–102

Sucgang R, Cheng G, Liu W, Lindsay R, Lu J, Muzny D, Shaulsky G, Loomis W, Gibbs R, Kuspa A (2003) Sequence and structure of the extrachromosomal palindrome encoding the ribosomal RNA genes in *Dictyostelium*. Nucleic Acids Res **31**:2361–2368

Taroncher-Oldenburg G, Kulis DM, Anderson DM (1997) Toxin variability during the cell cycle of the dinoflagellate *Alexandrium fundyense*. Limnol Oceanogr **42**:1178–1188

Taylor FJR, Hoppenrath M, Saldarriaga JF (2008) Dinoflagellate diversity and distribution. Biodivers Conserv **17**:407–418, http://dx.doi.org/10.1007/s10531-007-9258-3

Vogt VM, Braun R (1976) Structure of ribosomal DNA in *Physarum polycephalum*. J Mol Biol **106**:567–587

Wang L, Zhuang Y, Zhang H, Lin X, Lin S (2014) DNA barcoding species in *Alexandrium tamarense* complex using ITS and proposing designation of five species. Harmful Algae **31**:100–113, http://dx.doi.org/10.1016/j.hal.2013.10.013

Welker DL, Hirth KP, Williams KL (1985) Inheritance of extrachromosomal ribosomal DNA during the asexual life cycle of *Dictyostelium discoideum*: examination by use of DNA polymorphisms. Mol Cell Biol **5**:273–280

Zhang H, Campbell DA, Sturm NR, Lin S (2009) Dinoflagellate spliced leader RNA genes display a variety of sequences and genomic arrangements. Mol Biol Evol **26**:1757–1771, http://dx.doi.org/10.1093/molbev/msp083

Zhang S, Hemmerich P, Grosse F (2004) Nucleolar localization of the human telomeric repeat binding factor 2 (TRF2). J Cell Sci **117**:3935–3945, http://dx.doi.org/10.1242/jcs.01249